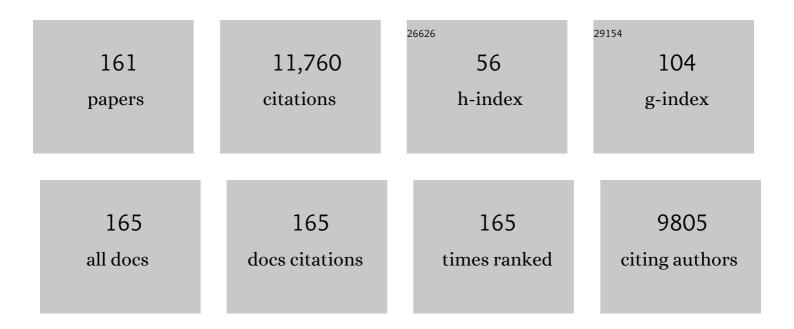
List of Publications by Year in descending order

Source: https://exaly.com/author-pdf/9109261/publications.pdf Version: 2024-02-01



PALLE FLORO

#	Article	IF	CITATIONS
1	Zeolite and molecular sieve synthesis. Chemistry of Materials, 1992, 4, 756-768.	6.7	1,362
2	The ammonia selective catalytic reduction activity of copper-exchanged small-pore zeolites. Applied Catalysis B: Environmental, 2011, 102, 441-448.	20.2	569
3	Cycloaddition of Biomass-Derived Furans for Catalytic Production of Renewable <i>p</i> -Xylene. ACS Catalysis, 2012, 2, 935-939.	11.2	400
4	Unconventional, Highly Selective CO ₂ Adsorption in Zeolite SSZ-13. Journal of the American Chemical Society, 2012, 134, 1970-1973.	13.7	363
5	Metalloenzyme-like catalyzed isomerizations of sugars by Lewis acid zeolites. Proceedings of the National Academy of Sciences of the United States of America, 2012, 109, 9727-9732.	7.1	354
6	Copper Coordination in Cu-SSZ-13 and Cu-SSZ-16 Investigated by Variable-Temperature XRD. Journal of Physical Chemistry C, 2010, 114, 1633-1640.	3.1	342
7	Production of renewable jet fuel range alkanes and commodity chemicals from integrated catalytic processing of biomass. Energy and Environmental Science, 2014, 7, 1500-1523.	30.8	342
8	Xylose Isomerization to Xylulose and its Dehydration to Furfural in Aqueous Media. ACS Catalysis, 2011, 1, 1724-1728.	11.2	301
9	SiOcntdotcntdotcntdot.HOSi Hydrogen Bonds in As-Synthesized High-Silica Zeolites. The Journal of Physical Chemistry, 1995, 99, 12588-12596.	2.9	233
10	Formation of [Cu ₂ O ₂] ²⁺ and [Cu ₂ O] ²⁺ toward C–H Bond Activation in Cu-SSZ-13 and Cu-SSZ-39. ACS Catalysis, 2017, 7, 4291-4303.	11.2	195
11	Characterization of the Extra-Large-Pore Zeolite UTD-1. Journal of the American Chemical Society, 1997, 119, 8474-8484.	13.7	168
12	SSZ-26 and SSZ-33: Two Molecular Sieves with Intersecting 10- and 12-Ring Pores. Science, 1993, 262, 1543-1546.	12.6	165
13	Structure of the Silica Phase Extracted from Silica/(TPA)OH Solutions Containing Nanoparticles. Journal of Physical Chemistry B, 2003, 107, 10006-10016.	2.6	164
14	Carbon Dioxide and Nitrogen Adsorption on Cation-Exchanged SSZ-13 Zeolites. Langmuir, 2013, 29, 832-839.	3.5	152
15	Bimetallic effects in the hydrodeoxygenation of meta-cresol on γ-Al2O3 supported Pt–Ni and Pt–Co catalysts. Green Chemistry, 2012, 14, 1388.	9.0	149
16	A DFT study of the acid-catalyzed conversion of 2,5-dimethylfuran and ethylene to p-xylene. Journal of Catalysis, 2013, 297, 35-43.	6.2	139
17	Probing Lewis Acid Sites in Sn-Beta Zeolite. ACS Catalysis, 2013, 3, 573-580.	11.2	137
18	CIT-1: A New Molecular Sieve with Intersecting Pores Bounded by 10- and 12-Rings. Journal of the American Chemical Society, 1995, 117, 3766-3779.	13.7	136

#	Article	IF	CITATIONS
19	Characterization and catalytic properties of MCM-56 and MCM-22 zeolites. Microporous and Mesoporous Materials, 2000, 40, 9-23.	4.4	136
20	Spontaneous Formation of Silica Nanoparticles in Basic Solutions of Small Tetraalkylammonium Cations. Journal of Physical Chemistry B, 2004, 108, 12271-12275.	2.6	136
21	The Role of Ru and RuO ₂ in the Catalytic Transfer Hydrogenation of 5â€Hydroxymethylfurfural for the Production of 2,5â€Dimethylfuran. ChemCatChem, 2014, 6, 848-856.	3.7	136
22	Elucidation of Diels–Alder Reaction Network of 2,5-Dimethylfuran and Ethylene on HY Zeolite Catalyst. ACS Catalysis, 2013, 3, 41-46.	11.2	131
23	Comparison of Homogeneous and Heterogeneous Catalysts for Glucoseâ€ŧoâ€Fructose Isomerization in Aqueous Media. ChemSusChem, 2013, 6, 2369-2376.	6.8	128
24	Lewis acidic zeolite Beta catalyst for the Meerwein–Ponndorf–Verley reduction of furfural. Catalysis Science and Technology, 2016, 6, 3018-3026.	4.1	125
25	The Synergy of the Support Acid Function and the Metal Function in the Catalytic Hydrodeoxygenation of m-Cresol. Topics in Catalysis, 2012, 55, 118-128.	2.8	123
26	Physical Basis for the Formation and Stability of Silica Nanoparticles in Basic Solutions of Monovalent Cations. Langmuir, 2005, 21, 8960-8971.	3.5	120
27	Renewable <i>p</i> â€Xylene from 2,5â€Dimethylfuran and Ethylene Using Phosphorusâ€Containing Zeolite Catalysts. ChemCatChem, 2017, 9, 398-402.	3.7	118
28	Renewable production of phthalic anhydride from biomass-derived furan and maleic anhydride. Green Chemistry, 2014, 16, 167-175.	9.0	114
29	Formation and Structure of Self-Assembled Silica Nanoparticles in Basic Solutions of Organic and Inorganic Cations. Langmuir, 2005, 21, 5197-5206.	3.5	104
30	Kinetic and Thermodynamic Studies of Silica Nanoparticle Dissolution. Chemistry of Materials, 2007, 19, 4189-4197.	6.7	104
31	Cascade of Liquidâ€Phase Catalytic Transfer Hydrogenation and Etherification of 5â€Hydroxymethylfurfural to Potential Biodiesel Components over Lewis Acid Zeolites. ChemCatChem, 2014, 6, 508-513.	3.7	104
32	Multiple-Quantum1H MAS NMR Studies of Defect Sites in As-Made All-Silica ZSM-12 Zeolite. Journal of the American Chemical Society, 2000, 122, 6659-6663.	13.7	103
33	A Model for the Structure of the Large-Pore Zeolite SSZ-31. Journal of the American Chemical Society, 1997, 119, 3732-3744.	13.7	100
34	MCM-47:Â A Highly Crystalline Silicate Composed of Hydrogen-Bonded Ferrierite Layers. Chemistry of Materials, 2000, 12, 2936-2942.	6.7	98
35	Cation-induced transformation of boron-coordination in zeolites. Physical Chemistry Chemical Physics, 2000, 2, 3091-3098.	2.8	92
36	Diels–Alder and Dehydration Reactions of Biomass-Derived Furan and Acrylic Acid for the Synthesis of Benzoic Acid. ACS Catalysis, 2015, 5, 6946-6955.	11.2	91

#	Article	IF	CITATIONS
37	Ethane and ethylene aromatization on zinc-containing zeolites. Catalysis Science and Technology, 2017, 7, 3562-3572.	4.1	91
38	ZKâ€5: A CO ₂ â€6elective Zeolite with High Working Capacity at Ambient Temperature and Pressure. ChemSusChem, 2012, 5, 2237-2242.	6.8	88
39	Challenges of and Insights into Acid-Catalyzed Transformations of Sugars. Journal of Physical Chemistry C, 2014, 118, 22815-22833.	3.1	88
40	Evolution of Self-Assembled Silicaâ^'Tetrapropylammonium Nanoparticles at Elevated Temperatures. Journal of Physical Chemistry B, 2005, 109, 12762-12771.	2.6	86
41	Catalytic dehydrogenation of propane over iron-silicate zeolites. Journal of Catalysis, 2014, 312, 263-270.	6.2	85
42	Experimental and computational studies on the adsorption of CO2 and N2 on pure silica zeolites. Microporous and Mesoporous Materials, 2014, 185, 157-166.	4.4	83
43	Photocatalytic degradation of organic molecules on mesoporous visible-light-active Sn(II)-doped titania. Journal of Catalysis, 2011, 281, 156-168.	6.2	82
44	Molecular Basis for the High CO ₂ Adsorption Capacity of Chabazite Zeolites. ChemSusChem, 2014, 7, 3031-3038.	6.8	81
45	Fe/γ-Al ₂ O ₃ and Fe–K/γ-Al ₂ O ₃ as reverse water-gas shift catalysts. Catalysis Science and Technology, 2016, 6, 5267-5279.	4.1	81
46	Silica Self-Assembly and Synthesis of Microporous and Mesoporous Silicates. Chemistry - A European Journal, 2006, 12, 2926-2934.	3.3	79
47	Kβ-Detected XANES of Framework-Substituted FeZSM-5 Zeolites. Journal of Physical Chemistry B, 2004, 108, 10002-10011.	2.6	77
48	Physicochemical Characterization of Zeolites SSZ-26 and SSZ-33. The Journal of Physical Chemistry, 1994, 98, 12040-12052.	2.9	70
49	Direct conversion of CO2 into methanol over promoted indium oxide-based catalysts. Applied Catalysis A: General, 2019, 583, 117144.	4.3	69
50	Nanoparticle Precursors and Phase Selectivity in Hydrothermal Synthesis of Zeolite β. Chemistry of Materials, 2008, 20, 5807-5815.	6.7	68
51	Effect of water treatment on Sn-BEA zeolite: Origin of 960Âcmâ^'1 FTIR peak. Microporous and Mesoporous Materials, 2015, 210, 69-76.	4.4	66
52	New Description of the Disorder in Zeolite ZSM-48. Journal of the American Chemical Society, 2002, 124, 13222-13230.	13.7	65
53	High-Temperature Dehydrogenation of BrÃ,nsted Acid Sites in Zeolites. Journal of the American Chemical Society, 2008, 130, 2460-2462.	13.7	64
54	Tunable Oleo-Furan Surfactants by Acylation of Renewable Furans. ACS Central Science, 2016, 2, 820-824.	11.3	64

#	Article	IF	CITATIONS
55	A simple model describes the PDF of a non-graphitizing carbon. Carbon, 2004, 42, 2041-2048.	10.3	63
56	Synthesis and characterization of pure-silica and boron-substituted SSZ-24 using N(16) methylsparteinium bromide as structure-directing agent. Microporous Materials, 1994, 3, 61-69.	1.6	61
57	Synthesis and Rietveld Refinement of the Small-Pore Zeolite SSZ-16. Chemistry of Materials, 1996, 8, 2409-2411.	6.7	58
58	Porous amorphous carbon models from periodic Gaussian chains of amorphous polymers. Carbon, 2005, 43, 3099-3111.	10.3	57
59	Variable anchoring of boron in zeolite beta. Microporous and Mesoporous Materials, 2005, 79, 215-224.	4.4	56
60	Low temperature catalytic NO oxidation over microporous materials. Journal of Catalysis, 2014, 311, 412-423.	6.2	55
61	Synthesis, characterization and photocatalytic properties of novel zinc germanate nano-materials. Journal of Solid State Chemistry, 2011, 184, 1054-1062.	2.9	52
62	Guestâ^'Host Interactions in As-Made Al-ZSM-12:Â Implications for the Synthesis of Zeolite Catalysts. Journal of Physical Chemistry B, 1999, 103, 10858-10865.	2.6	51
63	SnO _{<i>x</i>} –ZnGa ₂ O ₄ Photocatalysts with Enhanced Visible Light Activity. ACS Catalysis, 2011, 1, 923-928.	11.2	51
64	Zeolite beta mechanisms of nucleation and growth. Microporous and Mesoporous Materials, 2011, 142, 104-115.	4.4	51
65	NMR and SAXS Analysis of Connectivity of Aluminum and Silicon Atoms in the Clear Sol Precursor of SSZ-13 Zeolite. Chemistry of Materials, 2012, 24, 571-578.	6.7	51
66	Structure and Colloidal Stability of Nanosized Zeolite Beta Precursors. Langmuir, 2010, 26, 1260-1270.	3.5	47
67	A pair distribution function analysis of zeolite beta. Microporous and Mesoporous Materials, 2005, 77, 55-66.	4.4	46
68	Catalysis by Confinement: Enthalpic Stabilization of NO Oxidation Transition States by Micropororous and Mesoporous Siliceous Materials. Journal of Physical Chemistry C, 2013, 117, 20666-20674.	3.1	44
69	Oxidation of zeolite acid sites in NO/O2 mixtures and the catalytic properties of the new site in NO oxidation. Journal of Catalysis, 2015, 325, 68-78.	6.2	44
70	Reverse Water-Gas Shift Iron Catalyst Derived from Magnetite. Catalysts, 2019, 9, 773.	3.5	44
71	Synthesis and Characterization of Zincosilicates with the SOD Topology. Chemistry of Materials, 1994, 6, 2193-2199.	6.7	42
72	Photocatalytic Activity of Vanadium-Substituted ETS-10. Journal of Physical Chemistry C, 2007, 111, 7029-7037.	3.1	42

#	Article	IF	CITATIONS
73	Catalysis of the Diels–Alder Reaction of Furan and Methyl Acrylate in Lewis Acidic Zeolites. ACS Catalysis, 2017, 7, 2240-2246.	11.2	39
74	General Acid-Type Catalysis in the Dehydrative Aromatization of Furans to Aromatics in H-[Al]-BEA, H-[Fe]-BEA, H-[Ga]-BEA, and H-[B]-BEA Zeolites. Journal of Physical Chemistry C, 2017, 121, 13666-13679.	3.1	39
75	Nonâ€oxidative Coupling of Methane to Ethylene Using Mo ₂ C/[B]ZSMâ€5. ChemPhysChem, 2018, 19, 504-511.	2.1	38
76	Investigation of the Negative Thermal Expansion Mechanism of Zeolite Chabazite Using the Pair Distribution Function Method. Journal of Physical Chemistry B, 2005, 109, 9389-9396.	2.6	37
77	Mechanisms of Quick Zeolite Beta Crystallization. Chemistry of Materials, 2012, 24, 3621-3632.	6.7	36
78	Ironâ€Promotion of Silicaâ€5upported Copper Catalysts for Furfural Hydrodeoxygenation. ChemCatChem, 2016, 8, 3402-3408.	3.7	36
79	On the Structure–Property Relationships of Cationâ€Exchanged ZKâ€5 Zeolites for CO ₂ Adsorption. ChemSusChem, 2017, 10, 946-957.	6.8	36
80	Scaleup of a Single-Mode Microwave Reactor. Industrial & Engineering Chemistry Research, 2020, 59, 2516-2523.	3.7	36
81	Influence of Polymer Motion, Topology and Simulation Size on Penetrant Diffusion in Amorphous, Glassy Polymers:Â Diffusion of Helium in Polypropylene. Macromolecules, 2001, 34, 6107-6116.	4.8	35
82	Acylation of methylfuran with BrÃ,nsted and Lewis acid zeolites. Applied Catalysis A: General, 2018, 564, 90-101.	4.3	35
83	Title is missing!. Topics in Catalysis, 1999, 9, 1-11.	2.8	34
84	Effect of steam and CO ₂ on ethane activation over Zn-ZSM-5. Catalysis Science and Technology, 2018, 8, 358-366.	4.1	33
85	A General Method for Aluminum Incorporation into High-Silica Zeolites Prepared in Fluoride Media. Chemistry of Materials, 2016, 28, 638-649.	6.7	32
86	Synthesis, structure solution, and characterization of the aluminosilicate MCM-61: the first aluminosilicate clathrate with 18-membered rings. Microporous and Mesoporous Materials, 1999, 31, 61-73.	4.4	30
87	Self-Assembly and Phase Behavior of Germanium Oxide Nanoparticles in Basic Aqueous Solutions. Langmuir, 2007, 23, 2784-2791.	3.5	30
88	Ethane Dehydrogenation on Single and Dual Centers of Ga-modified Î ³ -Al ₂ O ₃ . ACS Catalysis, 2021, 11, 1380-1391.	11.2	30
89	A Spinel Oxynitride with Visible‣ight Photocatalytic Activity. ChemSusChem, 2010, 3, 814-817.	6.8	29
90	Production of <i>p</i> â€Methylstyrene and <i>p</i> â€Divinylbenzene from Furanic Compounds. ChemSusChem, 2017, 10, 91-98.	6.8	29

#	Article	IF	CITATIONS
91	Understanding the Correlation between Ga Speciation and Propane Dehydrogenation Activity on Ga/H-ZSM-5 Catalysts. ACS Catalysis, 2021, 11, 10647-10659.	11.2	29
92	Synthesis of (Alumino) Silicate Materials Using Organic Molecules and Self-Assembled Organic Aggregates as Structure-Directing Agents. Materials Research Society Symposia Proceedings, 1994, 346, 831.	0.1	28
93	Mobility of Li cations in X zeolites studied by solid-state NMR spectroscopy. Solid State Ionics, 1999, 118, 135-139.	2.7	28
94	Initial Stages of Self-Organization of Silicaâ^'Alumina Gels in Zeolite Synthesis. Langmuir, 2007, 23, 4532-4540.	3.5	28
95	Spatial Ordering of Organic and Inorganic Charge Centers in As-Made High-Silica Zeolites Determined by Multidimensional {1H} →2H CPMAS NMR Correlation Spectroscopy. Chemistry of Materials, 1998, 10, 4015-4024.	6.7	27
96	Framework modification of microporous silicates via gasâ€phase treatment with ZrCl4. Catalysis Letters, 1999, 62, 99-106.	2.6	27
97	Analysis of Ga coordination environment in novel spinel zinc gallium oxy-nitride photocatalysts. Journal of Materials Chemistry, 2010, 20, 9787.	6.7	27
98	Accessibility of lithium cations in high-silica zeolites investigated using the NMR paramagnetic shift effect of adsorbed oxygen. Microporous and Mesoporous Materials, 2000, 40, 25-34.	4.4	26
99	Understanding the differences between microporous and mesoporous synthesis through the phase behavior of silica. Microporous and Mesoporous Materials, 2006, 90, 102-111.	4.4	26
100	Thermodynamics of Silica Nanoparticle Self-Assembly in Basic Solutions of Monovalent Cations. Journal of Physical Chemistry C, 2008, 112, 14754-14761.	3.1	26
101	High-temperature dehydrogenation of defective silicalites. Microporous and Mesoporous Materials, 2010, 129, 156-163.	4.4	26
102	Radical Cation Intermediates in Propane Dehydrogenation and Propene Hydrogenation over H-[Fe] Zeolites. Journal of Physical Chemistry C, 2014, 118, 27292-27300.	3.1	26
103	Electronic and Geometric Properties of ETS-10:Â QM/MM Studies of Cluster Models. Journal of Physical Chemistry B, 2006, 110, 8959-8964.	2.6	25
104	Ga speciation in Ga/H-ZSM-5 by in-situ transmission FTIR spectroscopy. Journal of Catalysis, 2021, 393, 60-69.	6.2	25
105	Structure-Direction in Zeolite Synthesis. Topics in Inclusion Science, 1995, , 47-78.	0.5	25
106	The mechanical properties of siliceous ZSM-5 (MFI) crystals. Microporous and Mesoporous Materials, 2003, 57, 1-7.	4.4	24
107	Effects of Vanadium Substitution on the Structure and Photocatalytic Behavior of ETS-10. Journal of Physical Chemistry C, 2007, 111, 1776-1782.	3.1	24
108	Recent advances in zeolite science based on advance characterization techniques. Microporous and Mesoporous Materials, 2014, 189, 97-106.	4.4	24

#	Article	IF	CITATIONS
109	The role of barium cations in the synthesis of low-silica LTL zeolites. Microporous and Mesoporous Materials, 1999, 33, 97-113.	4.4	23
110	A fractal description of pore structure in block-copolymer templated mesoporous silicates. Microporous and Mesoporous Materials, 2010, 131, 204-209.	4.4	23
111	Formaldehyde–isobutene Prins condensation over MFI-type zeolites. Catalysis Science and Technology, 2018, 8, 5794-5806.	4.1	23
112	A visible light photocatalyst: effects of vanadium substitution on ETS-10. Physical Chemistry Chemical Physics, 2007, 9, 5096.	2.8	22
113	Investigation of the Structure of Platinum Clusters Supported in Zeolite Beta Using the Pair Distribution Function. Journal of Physical Chemistry C, 2007, 111, 8573-8579.	3.1	22
114	Highâ€Temperature Produced Catalytic Sites Selective for <i>n</i> â€Alkane Dehydrogenation in Acid Zeolites: The Case of HZSMâ€5. ChemCatChem, 2011, 3, 1333-1341.	3.7	21
115	Reactions of Propylene Oxide on Supported Silver Catalysts: Insights into Pathways Limiting Epoxidation Selectivity. Topics in Catalysis, 2012, 55, 3-12.	2.8	21
116	Zn-Promoted H-ZSM-5 for Endothermic Reforming of <i>n</i> -Hexane at High Pressures. Industrial & Engineering Chemistry Research, 2016, 55, 3930-3938.	3.7	21
117	Role of Boron in Enhancing the Catalytic Performance of Supported Platinum Catalysts for the Nonoxidative Dehydrogenation of <i>n</i> Butane. ACS Catalysis, 2020, 10, 1500-1510.	11.2	21
118	The promise of emptiness. Nature, 2006, 443, 757-758.	27.8	20
119	Identification of Mixed Valence Vanadium in ETS-10 Using Electron Paramagnetic Resonance, ⁵¹ V Solid-State Nuclear Magnetic Resonance, and Density Functional Theory Studies. Journal of Physical Chemistry C, 2009, 113, 10477-10484.	3.1	20
120	Solid-State Deuterium NMR Studies of Organic Molecules in the Tectosilicate Nonasil. Journal of Physical Chemistry B, 1998, 102, 2339-2349.	2.6	19
121	Zeolite atalyzed Formaldehyde–Propylene Prins Condensation. ChemCatChem, 2017, 9, 4417-4425.	3.7	19
122	Bioderived Muconates by Crossâ€Metathesis and Their Conversion into Terephthalates. ChemSusChem, 2018, 11, 773-780.	6.8	18
123	Ga ₂ O ₂ ²⁺ Stabilized by Paired Framework Al Atoms in MFI: A Highly Reactive Site in Nonoxidative Propane Dehydrogenation. ACS Catalysis, 2022, 12, 1775-1783.	11.2	18
124	High-Temperature Decomposition of BrÃ,nsted Acid Sites in Gallium-Substituted Zeolites. Journal of Physical Chemistry C, 2010, 114, 19395-19405.	3.1	17
125	The local and surface structure of ordered mesoporous carbons from nitrogen sorption, NEXAFS and synchrotron radiation studies. Microporous and Mesoporous Materials, 2006, 92, 81-93.	4.4	16
126	Synthetic Glycolysis. ChemSusChem, 2010, 3, 1237-1240.	6.8	16

#	Article	IF	CITATIONS
127	H ₂ Adsorption on Cu(I)–SSZ-13. Journal of Physical Chemistry C, 2018, 122, 540-548.	3.1	16
128	Chemical diversity of zeolite catalytic sites. AICHE Journal, 2008, 54, 1402-1409.	3.6	15
129	Lewis Acid Site and Hydrogen-Bond-Mediated Polarization Synergy in the Catalysis of Diels–Alder Cycloaddition by Band-Gap Transition-Metal Oxides. ACS Catalysis, 2019, 9, 701-715.	11.2	15
130	Photocatalytic oxidation of ethylene by ammonium exchanged ETS-10 and AM-6. Applied Catalysis B: Environmental, 2009, 88, 232-239.	20.2	13
131	Structure Analysis and Photocatalytic Properties of Spinel Zinc Gallium Oxonitrides. Chemistry - A European Journal, 2011, 17, 12417-12428.	3.3	13
132	Analysis of visible-light-active Sn(ii)–TiO2 photocatalysts. Physical Chemistry Chemical Physics, 2013, 15, 6185.	2.8	13
133	Spatial Correlation of Charge Centers in the Tectosilicate Nonasil Determined by Multidimensional {1H} →2H CPMAS NMR Correlation Spectroscopy. Journal of the American Chemical Society, 1998, 120, 2482-2483.	13.7	12
134	Formation and evolution of naphthalene radical cations in thermally treated H-ZSM-5 zeolites. Microporous and Mesoporous Materials, 2012, 155, 82-89.	4.4	12
135	Propane Dehydrogenation over Extra-Framework In(I) in Chabazite Zeolites. Chemical Science, 2022, 13, 2954-2964.	7.4	12
136	Paramagnetic Effect of Oxygen in the 23Na MAS NMR and 23Na MQMAS NMR Spectroscopy of Zeolite LiNaX. Journal of Physical Chemistry B, 2001, 105, 5883-5886.	2.6	11
137	Electron Transfers Induced by <i>t</i> -Stilbene Sorption in Acidic Aluminum, Gallium, and Boron Beta (BEA) Zeolites. Journal of Physical Chemistry C, 2012, 116, 14480-14490.	3.1	11
138	Catalytic n-pentane conversion on H-ZSM-5 at high pressure. New Journal of Chemistry, 2016, 40, 4245-4251.	2.8	11
139	Selective Synthesis of 4,4′-Dimethylbiphenyl from 2-Methylfuran. ACS Sustainable Chemistry and Engineering, 2021, 9, 3316-3323.	6.7	11
140	Zeolite MCM-22 Supported Heterogeneous Chromium Catalyst for Ethylene Polymerization. Catalysis Letters, 2003, 88, 227-229.	2.6	10
141	Structural comparison of two EUO-type zeolites investigated by neutron diffraction. Microporous and Mesoporous Materials, 2004, 71, 125-133.	4.4	9
142	Effects of Zeolite Structures, Exchanged Cations, and Bimetallic Formulations on the Selective Hydrogenation of Acetylene Over Zeolite-Supported Catalysts. Catalysis Letters, 2009, 130, 380-385.	2.6	9
143	Linking low and high temperature NO oxidation mechanisms over BrÃ,nsted acidic chabazite to dynamic changes of the active site. Journal of Catalysis, 2020, 389, 195-206.	6.2	9
144	Hydrothermal synthesis of alkali-free chabazite zeolites. Journal of Porous Materials, 2020, 27, 1481-1489.	2.6	9

#	Article	IF	CITATIONS
145	Effect of Al on Zeolite Beta Solid State Chemistry. Topics in Catalysis, 2012, 55, 1332-1343.	2.8	8
146	2Hâ^'{H} CPMAS NMR of Guestâ^'Host Species in Zeolites:  An Experimental Study. Journal of Physical Chemistry B, 1999, 103, 5920-5927.	2.6	7
147	Grand canonical Monte Carlo simulation of adsorption of nitrogen and oxygen in realistic nanoporous carbon models. AICHE Journal, 2011, 57, 1496-1505.	3.6	6
148	Improved slit-shaped microseparator and its integration with a microreactor for modular biomanufacturing. Green Chemistry, 2021, 23, 3700-3714.	9.0	6
149	Comparison of 4,4′-Dimethylbiphenyl from Biomass-Derived Furfural and Oil-Based Resource: Technoeconomic Analysis and Life-Cycle Assessment. Industrial & Engineering Chemistry Research, 2022, 61, 8963-8972.	3.7	6
150	Introduction to the Structural Chemistry of Zeolites. , 2003, , .		5
151	Oxidative coupling of 2-methyl furoate: A scalable synthesis of dimethyl 2,2'-bifuran-5,5'-dicarboxylate. Applied Catalysis A: General, 2021, 619, 118138.	4.3	5
152	Indirect Fourier Transform and Model Fitting of Small Angle Neutron Scattering from Silica Nanoparticles. Particle and Particle Systems Characterization, 2010, 27, 89-99.	2.3	4
153	On the Mechanism of Ammonia SCR over Cu- and Fe-Containing Zeolite Catalysts. Structure and Bonding, 2018, , 155-178.	1.0	4
154	Nickel-Loaded SSZ-13 Zeolite-Based Sensor for the Direct Electrical Readout Detection of NO ₂ . Industrial & Engineering Chemistry Research, 2021, 60, 14371-14380.	3.7	4
155	Electron Transfers Under Confinement in Channel-Type Zeolites. , 2019, , 249-271.		3
156	Selective and Efficient Production of Biomass-Derived Vinylfurans. ACS Sustainable Chemistry and Engineering, 2020, 8, 11930-11939.	6.7	3
157	Olefin methylation over iron zeolites and the methanol to hydrocarbons reaction. Applied Catalysis A: General, 2022, 641, 118645.	4.3	3
158	Externally directed assembly of disk-shaped zeolite particles by an electric field. Journal of Materials Research, 2011, 26, 215-222.	2.6	2
159	Carbocation-Mediated Cyclization of Trienes in Acid Zeolites. Journal of Physical Chemistry A, 2021, 125, 4062-4069.	2.5	2
160	Pair Distribution Function as a Probe for Zeolite Structures. Materials Research Society Symposia Proceedings, 2004, 840, Q1.4.1.	0.1	0
161	Intermolecular Forces in Zeolite Adsorption and Catalysis. , 2009, , 239-261.		0